

Increased Alternative Lengthening of Telomere Phenotypes of Telomerase-negative Immortal Cells upon Trichostatin – A Treatment

A RA JUNG^{1,4}, JEONG EUN YOO², YHONG-HEE SHIM¹, YE-NA CHOI¹, HEI-CHEUL JEUNG^{3,4},
HYUN CHEOL CHUNG^{3,4}, SUN YOUNG RHA^{3,4} and BONG-KYEONG OH¹

¹Department of Bioscience and Biotechnology, Brain Korea 21 Division of Bioscience and Biotechnology,
Konkuk University, Seoul, Republic of Korea;

Departments of ²Pathology and ³Internal Medicine,
Yonsei University College of Medicine, Seoul, Republic of Korea;

⁴Cancer Metastasis Research Center, Brain Korea 21 Project for Medical Science,
Yonsei University College of Medicine, Seoul, Republic of Korea

Abstract. Human immortal cells maintain their telomeres either by telomerase or by alternative lengthening of telomeres (ALT) that is based on homologous telomeric recombination. Previous studies showed that the ALT mechanism is activated in non-ALT cells when heterochromatic features are reduced. In this study, we examined the ALT phenotypes of ALT cells after treatment with trichostatin-A (TSA), which is an inhibitor of histone deacetylases and causes global chromatin decondensation. The ALT cells remained telomerase-negative after TSA treatment. ALT-associated promyelocytic leukemia (PML) nuclear bodies and telomere sister chromatid exchanges, typical ALT phenotypes, markedly increased in the TSA-treated cells, while the telomere length remained unchanged. In addition, telomerase expression in the ALT cells suppressed TSA-mediated ALT phenotype enhancement. Our results show that certain ALT phenotypes become more pronounced when chromatin is decondensed, and also suggest that the ALT mechanism may compete with telomerase for telomere maintenance in cells that lack heterochromatin.

Correspondence to: Bong-Kyeong Oh, Ph.D., Department of Bioscience and Biotechnology, Brain Korea 21 Division of Bioscience and Biotechnology, Konkuk University, Seoul 143-701, Republic of Korea. E-mail: boh0318@konkuk.ac.kr and Sun Young Rha, MD, Ph.D., Department of Internal Medicine, Yonsei University College of Medicine, Seoul 120-752, Republic of Korea. E-mail: rha7655@yuhs.ac

Key Words: Telomere, chromatin, telomerase, trichostatin A, ALT mechanism, recombination.

Most tumor cells utilize telomerase for the purpose of telomere maintenance to gain cellular immortality (1). The other mechanism that maintains telomere length is the alternative lengthening of telomeres (ALT). In fact, some tumor cells maintain their telomere length in the absence of detectable telomerase activity and have the capacity to undergo infinite division (2). These so-called ALT cells are characterized by heterogeneous telomere lengths that range from 3 to 50 kb (2), the formation of ALT-associated promyelocytic leukemia (PML) bodies (APBs) (3), and frequent post-replicative exchanges between telomeric repeats, as shown by telomere sister chromatid exchange (T-SCE) (4). It has been suggested that the telomere length of ALT cells is maintained by a mechanism that is based on homologous telomeric recombination (5).

Heterochromatic features, such as a high level of DNA methylation, the tri-methylation of histone 3 Lys 9 (H3K9) and histone 4 Lys 20 (H4K20), are found in telomeric and sub-telomeric chromatins (6). When the chromatin structure of a telomere is dysregulated, regulation of the telomere length seems to be affected. For instance, cells that were derived from a histone methyltransferase-knockout mouse exhibited lower H3K9 and H4K20 tri-methylation at the telomeres, frequent telomeric recombination, and aberrant telomere elongation (7, 8). Similar phenotypes were also observed in DNA methyltransferase-deficient cells (9). In addition, the treatment of human cancer cells that were telomerase-positive with DNA-demethylating drugs increased their telomere recombination, thereby facilitating telomere elongation (10). These studies showed that the loss of heterochromatic features resulted in the emergence of an ALT mechanism in telomerase-positive cells and mouse somatic cells.

The question may arise as to whether or not the epigenetic modifications have any influence on the ALT mechanism in ALT cells. In this study, we investigated the ALT phenotypes of ALT cells whose chromatin structures were relaxed. To bring about chromatin decondensation, the ALT cells were treated with trichostatin-A (TSA), which is a histone deacetylase inhibitor, thereby leading to global histone hyperacetylation (11, 12). We then examined the changes that occurred in the ALT phenotypes such as APBs, T-SCEs, and telomere length upon TSA treatment of the ALT cells. Our results showed that certain ALT phenotypes became more evident in the TSA-treated ALT cells and that the introduction of telomerase into the ALT cells reduced TSA-mediated ALT phenotype enhancement.

Materials and Methods

Cell culture and establishment of GM847 stably-expressing human telomerase reverse transcriptase (hTERT). WI38VA13 and GM847 cells, which were derived from lung and skin fibroblasts, respectively, were purchased from the Korean Cell Line Bank (Seoul, Korea) and the Coriell Institute (Camden, NJ, USA), respectively. GM847/hTERT and GM847/vector cells were established by infection with lenti-hTERT and lenti-enhanced green fluorescence protein (EGFP) viral supernatant, respectively, which were purchased from Applied Biological Materials Inc. (Cat. G200; ABM, BC, Canada).

Western blot analysis. For the detection of acetyl histones, cells were lysed in sodium dodecyl sulfate (SDS) lysis buffer (50 mM Tris-Cl [pH 7.5], 1% SDS, and 10% glycerol) and sonicated to fractionate the genomic DNA. The protein concentration was determined using a DC-protein assay kit (Bio-Rad, Hercules, CA, USA). Proteins (15 µg) were separated on 12.5% native polyacrylamide gels and then transferred to membranes. The membranes were incubated with primary antibodies against H3K9 (1:500; Millipore, Billerica, MA, USA) for 2 h, H4K8 (1:1,000; Cell Signaling, Danvers, MA, USA) for 2 h, and glyceraldehydes-3-phosphate dehydrogenase (1:20,000; GAPDH; Abcam, Cambridge, MA, USA) for 1 h. For the detection of hTERT, the cells were lysed with RIPA lysis buffer, and the hTERT protein was detected using a rabbit monoclonal antibody to hTERT (1:1,000; Epitomics, Burlingame, CA, USA).

Quantitative real-time reverse transcription-polymerase chain reaction (RT-PCR) for hTERT. Real-time RT-PCR for hTERT mRNA was performed with 1× Power SYBR® green PCR master mix (Applied Biosystems, Foster City, CA, USA). The sequences of the hTERT primers have been described previously (13). GAPDH amplification was performed using a Taqman GAPDH gene expression assay® (Applied Biosystems).

Detection of APBs. APBs were detected by fluorescence *in situ* hybridization (FISH) combined with immunofluorescence as described in a previous report (14). Briefly, cells that were treated with TSA (Sigma, St. Louis, MO, USA) at a final concentration of 100 nM or 200 nM for 48 h were permeated, fixed, and permeated once again. The hybridization was performed with Cy3 conjugated-

(C₃TA₂)₃ peptide nucleic acid (PNA) probe (Panagene, Daejeon, Korea), and then the cells were incubated with a PML antibody (1:500; Abcam) at 4°C overnight. After incubation with a mixture of Alexa Fluor 488 goat anti-rabbit IgG (1:400; Invitrogen, Carlsbad, CA, USA) and 4',6-diamidino-2-phenylindole (DAPI), the cells were then mounted in anti-fading medium (Invitrogen). Images were captured by using a confocal microscope (Carl Zeiss, Oberkochen, Germany) and analyzed with Image-Pro® Plus (Media Cybernetics, Bethesda, MD, USA).

Detection of telomere length. Telomere length was determined using a quantitative telomeric fluorescence *in situ* hybridization (Q-FISH) method, as previously described (15). Briefly, cells were treated with TSA at a final concentration of 100 nM or 200 nM, and colcemid was added to the culture after 41 h (2 µg/ml for GM847, GM847/vector, and GM847/hTERT cells, and 10 µg/ml for WI38VA13 cells). The cells were harvested after 7 h, swelled in hypotonic buffer, and fixed in fixative solution. The cell suspensions were dropped onto coated slides and fixed twice. Then, hybridization was performed, as described in the APB methods. After extensive washing, the slides were stained with DAPI and covered with antifade solution (Invitrogen). Images of metaphases were captured by using a fluorescence microscope (Olympus, Tokyo, Japan), and the fluorescence intensities of the telomeres were quantified using Image-Pro® Plus (Media Cybernetics).

Chromosome orientation-FISH. The T-SCE frequency was measured by chromosome orientation FISH (CO-FISH) by a previously described method, with a slight modification (16). Cells were treated with TSA, and 24 h later, 5-bromo-2-deoxyuridine (BrdU; Sigma) was added to the culture at a final concentration of 10 µM for 24 h, which allowed a single cell-cycle to occur; colcemid was then added, as described in the Q-FISH analysis. Cells were harvested, and metaphases were prepared on poly-D lysine coated coverslips, as described in the Q-FISH methods. Coverslips were incubated with 0.5 mg/ml RNase A (Sigma) at 37°C for 10 min, and then stained with 10 µg/ml Hoechst 33258 in 2× saline-sodium citrate (SSC), at room temperature for 10 min. Coverslips were then mounted with 1× phosphate buffered saline (PBS) and exposed to UV light for 30 min. This was followed by fixation, washing, and dehydration. Hybridization was then performed as described in the FISH analysis procedure without the denaturation step. Images were captured on a fluorescence microscope (Olympus) and T-SCEs were quantified using Image-Pro® Plus (Media Cybernetics).

Statistical analysis. Statistical analyses were performed using the SPSS 13.0 software (SPSS, Chicago, IL, USA) and assessed by using the Student's *t*-test and the χ^2 -test. Significance was defined as a *p*-value of less than 0.05.

Results

TSA induces histone acetylation but hTERT expression remains silenced in GM847 cells. To examine histone acetylation in ALT cells, GM847 cells were initially treated with TSA at different concentrations and durations. Immunoblotting showed that histone acetylation at H3K9 and H4K8 was induced at 100 nM TSA and that the level of histone acetylation persisted without a significant decrease for

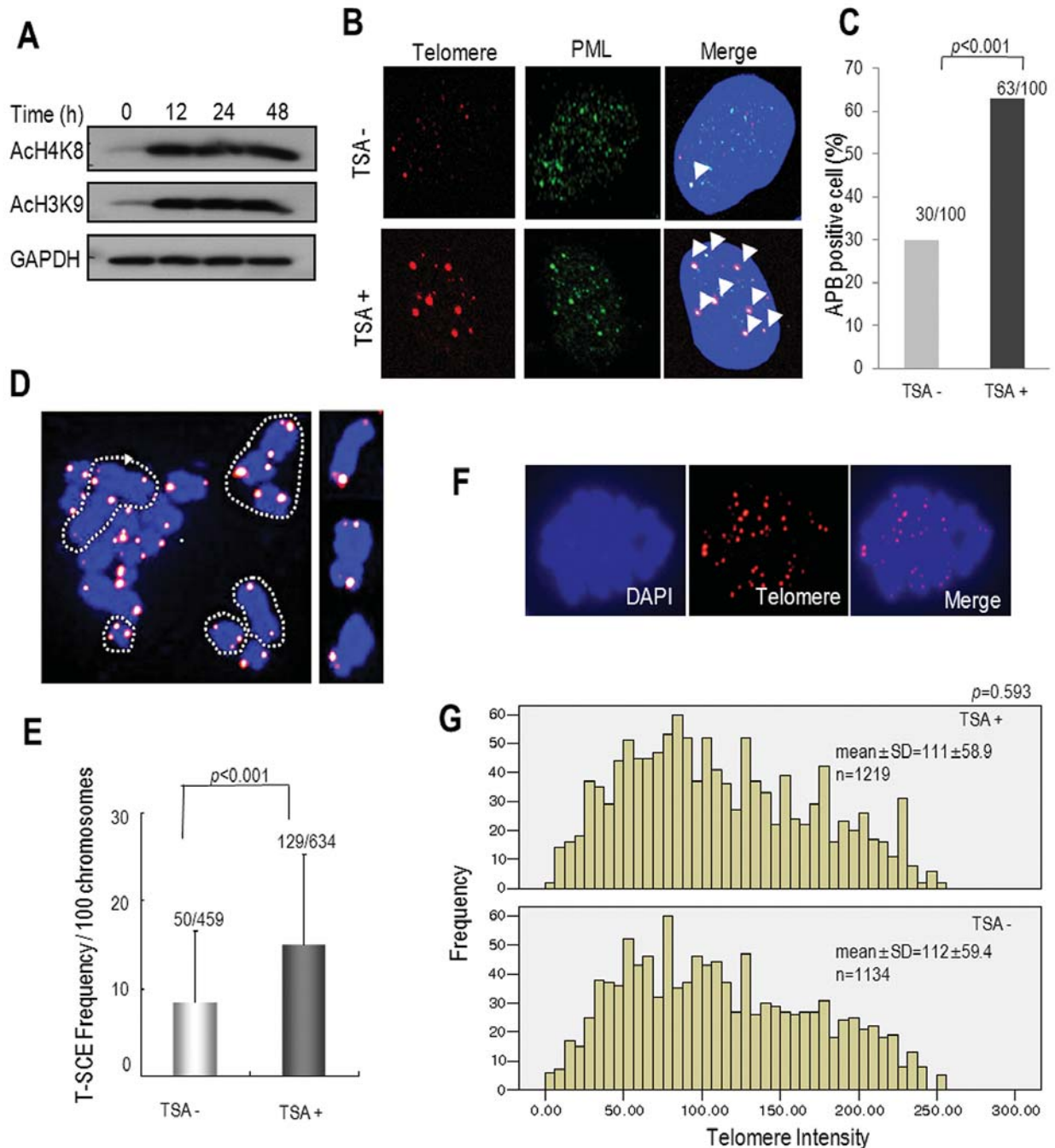


Figure 1. Alternative lengthening of telomere (ALT) phenotypes of GM847 cells after trichostatin-A (TSA) treatment. **A**: Histone acetylation in GM847 cells after TSA treatment. GM847 cells that were treated with 100 nM TSA for the indicated times were subjected to immunoblotting to determine the acetylation of histone H3 Lys9 (AcH3K9) and H4 Lys8 (AcH4K8). Glyceraldehydes-3-phosphate dehydrogenase (GAPDH) was used as a loading control. **B**: ALT-associated promyelocytic leukemia (PML) body (APB) formation in GM847 cells. GM847 cells treated with 100 nM TSA for 48 h were hybridized with a Cy3-conjugated peptide, nucleic acid telomere probe and immunostained with an anti-PML antibody. APBs were analyzed by merging the signals for telomere and PML in the nucleus. Representative images are shown, and the APBs are indicated by arrows. **C**: Quantification of the data represented in B. APBs were examined across 100 cells in two independent experiments. p -Value by χ^2 -test. **D**: Detection of telomere sister chromatid exchanges (T-SCEs) in GM847 cells after TSA treatment. A representative image of chromosome orientation fluorescence in situ hybridization analyses is shown on the left, where chromosomes with T-SCEs are indicated with the dotted lines. Representative T-SCE-positive chromosomes are shown on the right. **E**: Quantification of the data represented in D. Error bars indicate SD from three independent experiments (p -value by χ^2 -test). **F**: Representative telomere FISH images of GM847 cells. **G**: Distribution of telomere signals in TSA-treated and untreated GM847 cells (p -value by Student's t -test).

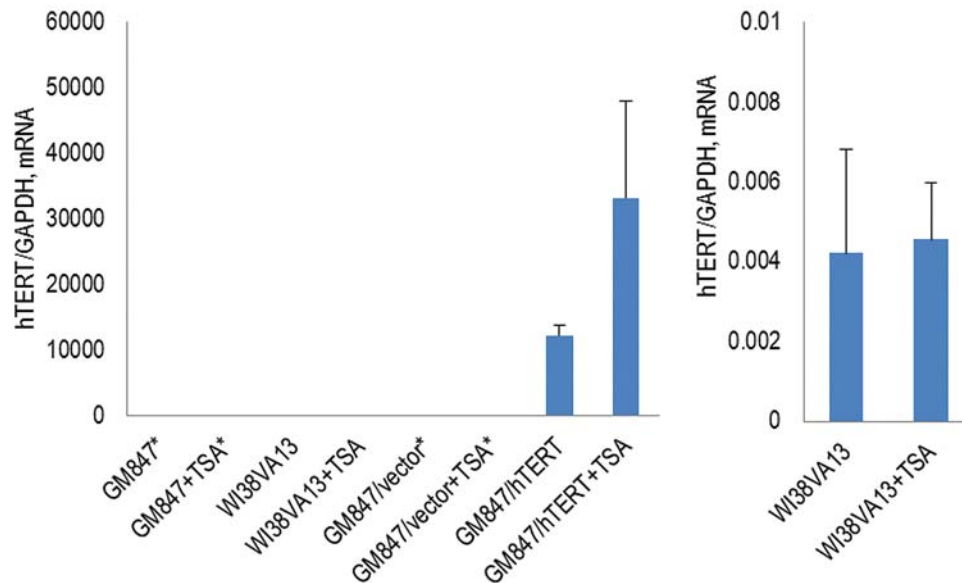


Figure 2. Comparison of *hTERT* mRNA levels in mock-treated and trichostatin-A (TSA)-treated alternative lengthening of telomeres cells. TSA treatment was as follows: GM847 cells were treated with 100 nM TSA for 48 h and WI38V13, GM847/vector, and GM847/hTERT cells were treated with 200 nM TSA for 48 h. Samples with the asterisks exhibited no expression of *hTERT* mRNA. WI38VA13 cells expressed a minimum level of *hTERT* mRNA, as shown on the right of the graph. The error bars indicate SD from two independent experiments.

at least 48 h (Figure 1A). Next, we examined the mRNA of *hTERT*, which is a catalytic component of telomerase, to find out if TSA induces *hTERT* expression in GM847 cells. Cells that were treated with 100 nM TSA for 48 h were subjected to quantitative RT-PCR. *hTERT* mRNA remained silenced in both the TSA-treated and untreated cells (Figure 2), suggesting that TSA-induced histone acetylation exerts no influence on *hTERT* gene expression in the GM847 cells. These results suggest that TSA treatment induced histone acetylation; however, the GM847 cells remained telomerase- negative.

TSA increases APB formation in GM847 cells. To investigate whether TSA influences the ALT phenotype of GM847 cells, APBs detected by merging the telomere and PML protein staining were examined in the cells treated with 100 nM TSA for 48 h. We analyzed 100 cells from two independent experiments. To minimize the inclusion of non-specific spots, APBs of $\geq 0.1 \mu\text{m}^3$ in size were counted using Image-Pro® Plus (Media Cybernetics). The number of APBs increased markedly in the TSA-treated cells ($p < 0.001$; Figures 1B and C). Out of 100 TSA-treated cells, 63 cells were APB-positive and seven cells contained ≥ 6 APBs/cell. Some telomere spots were apparently large with strong intensities, while PML signals seemed to remain unaffected by the treatment of TSA, and strong telomere spots were mostly co-localized with PML bodies (Figure 1B). On the other hand, in the untreated cells, a smaller fraction of the cells were APB-

positive (30/100) and none of those contained more than six APBs per cell. These results show that TSA treatment increases the formation of APBs and enlarges some APBs in GM847 cells.

TSA treatment increases T-SCE frequency in GM847 cells but telomere length remains unchanged. CO-FISH analysis was used to detect SCE events at telomeres. Metaphases were prepared from cells treated with TSA, followed by telomere-FISH analysis, and chromosomes with T-SCEs were counted (Figure 1D). T-SCEs were more frequently observed in TSA-treated cells; T-SCEs were detected in 20% of the chromosomes (129/634) in the TSA-treated cells, whereas the control cells had T-SCEs only in 11% of their chromosomes (50/459; $p < 0.001$). These results show that TSA induces SCE events at telomeres in GM847 cells (Figures 1D and E).

We further investigated whether TSA treatment leads to any changes in telomere length. Telomere length was examined by performing Q-FISH analysis (Figures 1F and G). There was no noticeable difference in the telomere length between the TSA-treated and untreated cells; the mean telomere intensity, which is proportional to the length, was 111 ± 58.9 in the TSA-treated cells and 112 ± 59.4 in the untreated cells (Figure 1G; $p = 0.593$). We also looked at the distribution of telomere intensity and found a similar pattern in both the TSA-treated and untreated cells (Figure 1G). It

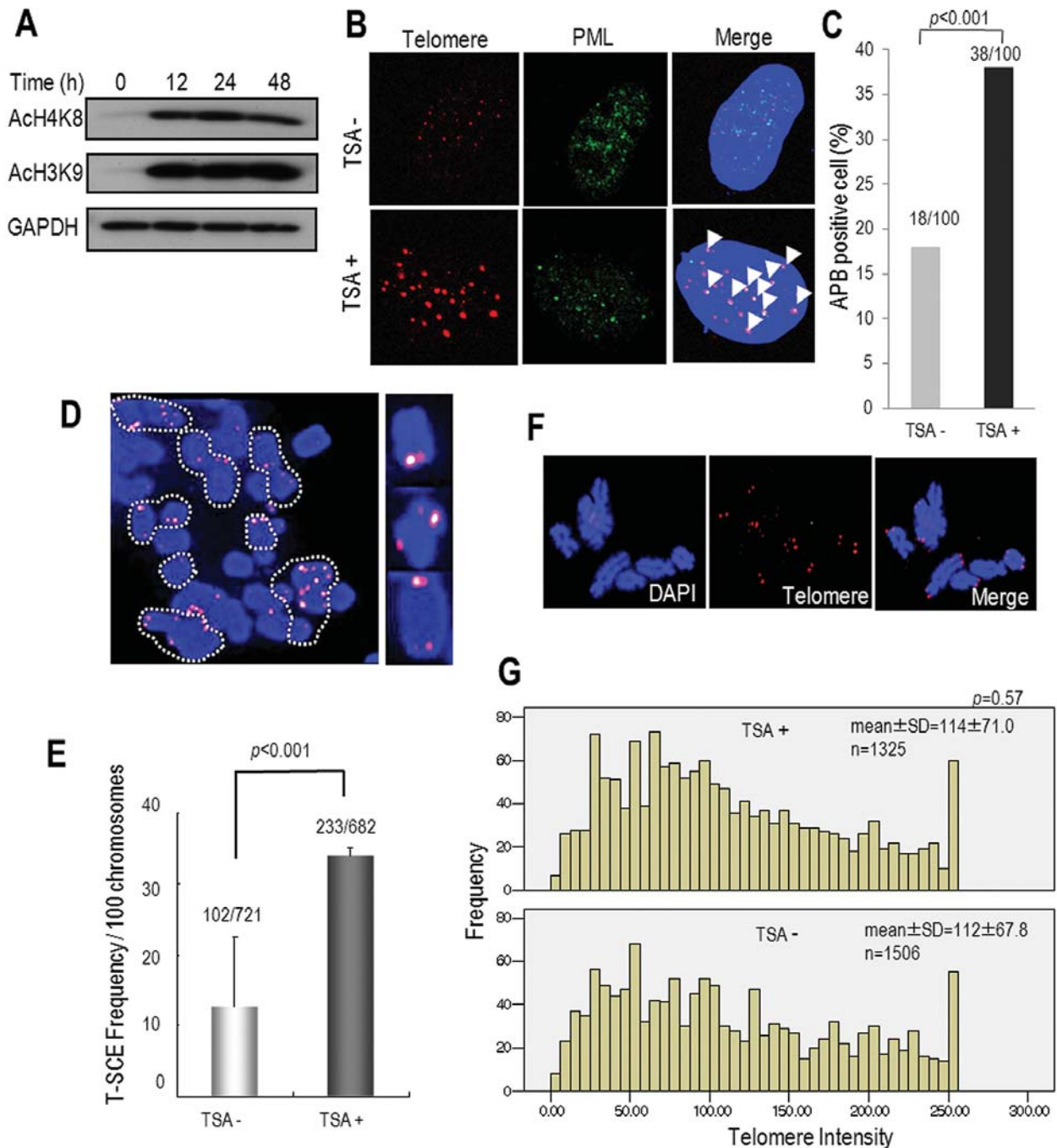


Figure 3. Alternative lengthening of telomere (ALT) phenotypes of WI38VA13 cells after trichostatin-A (TSA) treatment. **A**: Histone acetylation in WI38VA13 cells upon TSA treatment. WI38VA13 cells treated with 200 nM of TSA for the indicated times were used in the immunoblot using anti-acetyl H3K9 and anti-acetyl H4K8 antibodies. Glyceraldehydes-3-phosphate dehydrogenase was used as the loading control. **B**: ALT-associated promyelocytic leukemia (PML) body (APB) formation in WI38VA13 cells upon TSA treatment. WI38VA13 cells that were treated with 200 nM TSA for 48 h were hybridized with a telomere probe and immunostained with an anti-rabbit PML antibody. APBs were detected by merging the signals for telomere and PML in the nucleus, which had been stained with 4',6-diamidino-2-phenylindole (DAPI). APBs of $\geq 0.1 \mu\text{m}^3$ in size were counted using Image-Pro® Plus (Media Cybernetics) (arrows indicate the APBs). **C**: Quantification of APBs represented in **B**. APBs were examined across 100 cells in three independent experiments. p -Value by χ^2 -test. **D**: Detection of telomere sister chromatid exchanges (T-SCEs) in WI38VA13 cells after TSA treatment. Chromosomes with T-SCE are indicated with the dotted lines. Representative T-SCE-positive chromosomes are shown on the right. **E**: Quantification of T-SCE frequencies represented in **D**. Mean values were derived from two independent experiments (p -value by χ^2 -test). **F**: Representative telomere FISH images of WI38VA13 cells. **G**: Distribution of telomere signals in TSA-treated and untreated WI38VA13 cells (p -value by Student's t -test).

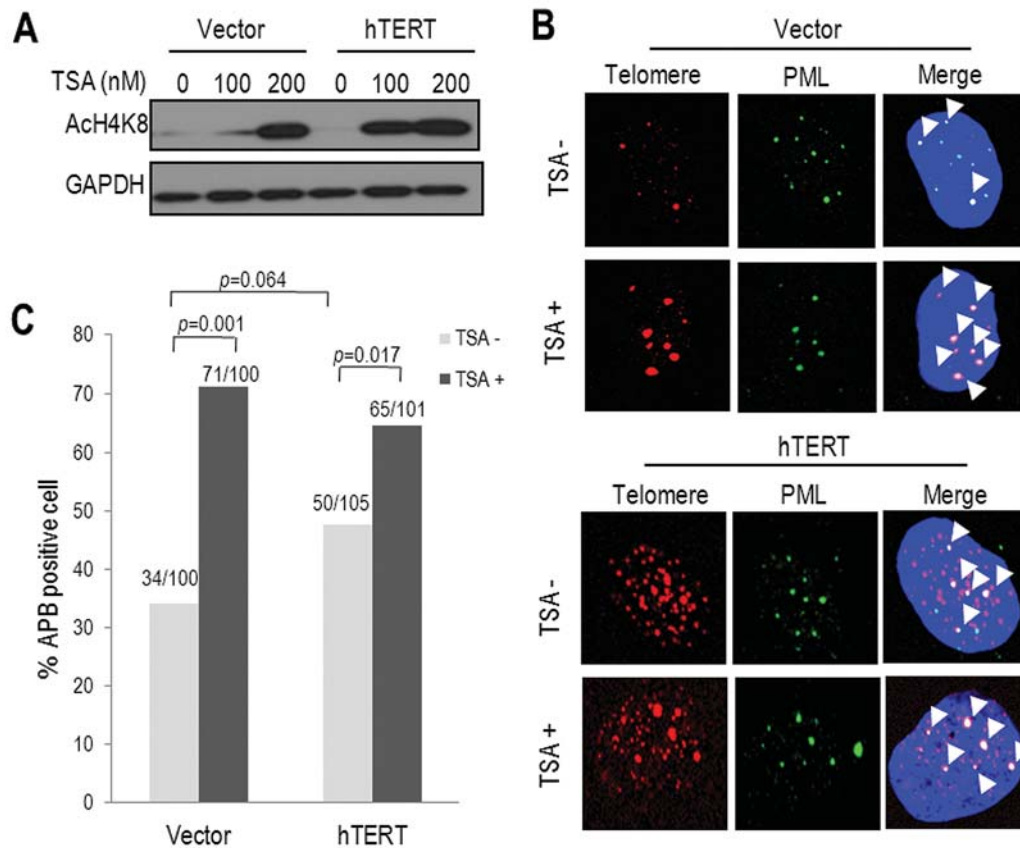


Figure 4. Alternative lengthening of telomere (ALT) phenotypes of GM847/hTERT cells upon trichostatin-A (TSA) treatment. **A:** Histone acetylation of GM847/hTERT and GM847/vector cells upon TSA treatment. Cells treated with the indicated concentration of TSA for 48 h were subjected to immunoblotting to determine the acetylation of histone H4 Lys8. Glyceraldehydes-3-phosphate dehydrogenase was used as a loading control. **B:** Detection of ALT-associated promyelocytic leukemia (PML) bodies (APBs). Cells that were treated with 200 nM TSA for 48 h were hybridized with a telomere probe, followed by immunostaining with an anti-rabbit PML antibody (the arrows indicate APBs). **C:** Quantification of the data represented in B. A minimum of 100 cells were examined from two independent experiments. APBs of $\geq 0.1 \mu\text{m}^3$ in size were counted using Image-Pro® Plus (Media Cybernetics). A χ^2 -test was used to compare the APB frequencies.

is not clear why the telomere length was not affected, although APBs and T-SCEs were obviously increased after treatment with TSA. In general, long-term monitoring is required for the detection of changes in the telomere length from ALT cells in which the telomere maintenance mechanism is disrupted (17, 18). We, thus, speculated that 48 h of TSA treatment might not have been sufficient to show a difference in the telomere length. Taken together, APBs and T-SCEs seem to be more prevalent in ALT cells when chromatin structure is less condensed. The results of APB and quantitative FISH analyses showed that the emergence of strong telomere spots at PML bodies in the TSA-treated cells were unlikely to be due to lengthened telomeres. It is thought that some telomeres in different chromosomes seem to be assembled at PML bodies upon TSA treatment.

Characteristics of WI38VA13 cells upon TSA treatment. To analyze whether the phenotypes that were observed in GM847 cells upon TSA treatment are the general features of ALT cells, we performed additional experiments with another well-characterized ALT cell line, WI38VA13, which is an SV40-immortalized lung fibroblast cell line. The TSA treatment was set at 200 nM for 48 h because histone acetylation was strongly induced under this condition (Figure 3A). WI38VA13 cells, which contained a tiny amount of *hTERT* mRNA in the untreated cells, showed no increase in *hTERT* mRNA upon TSA treatment (Figure 2). APBs were detected more frequently in the TSA-treated cells (38/100) than in untreated cells (18/100; $p<0.001$; Figures 3B and C). Large size APBs were also frequently seen in the TSA-treated WI38VA13 cells (Figure 3B), as in the case of the GM847 cells. On the other hand, in the untreated cells, a

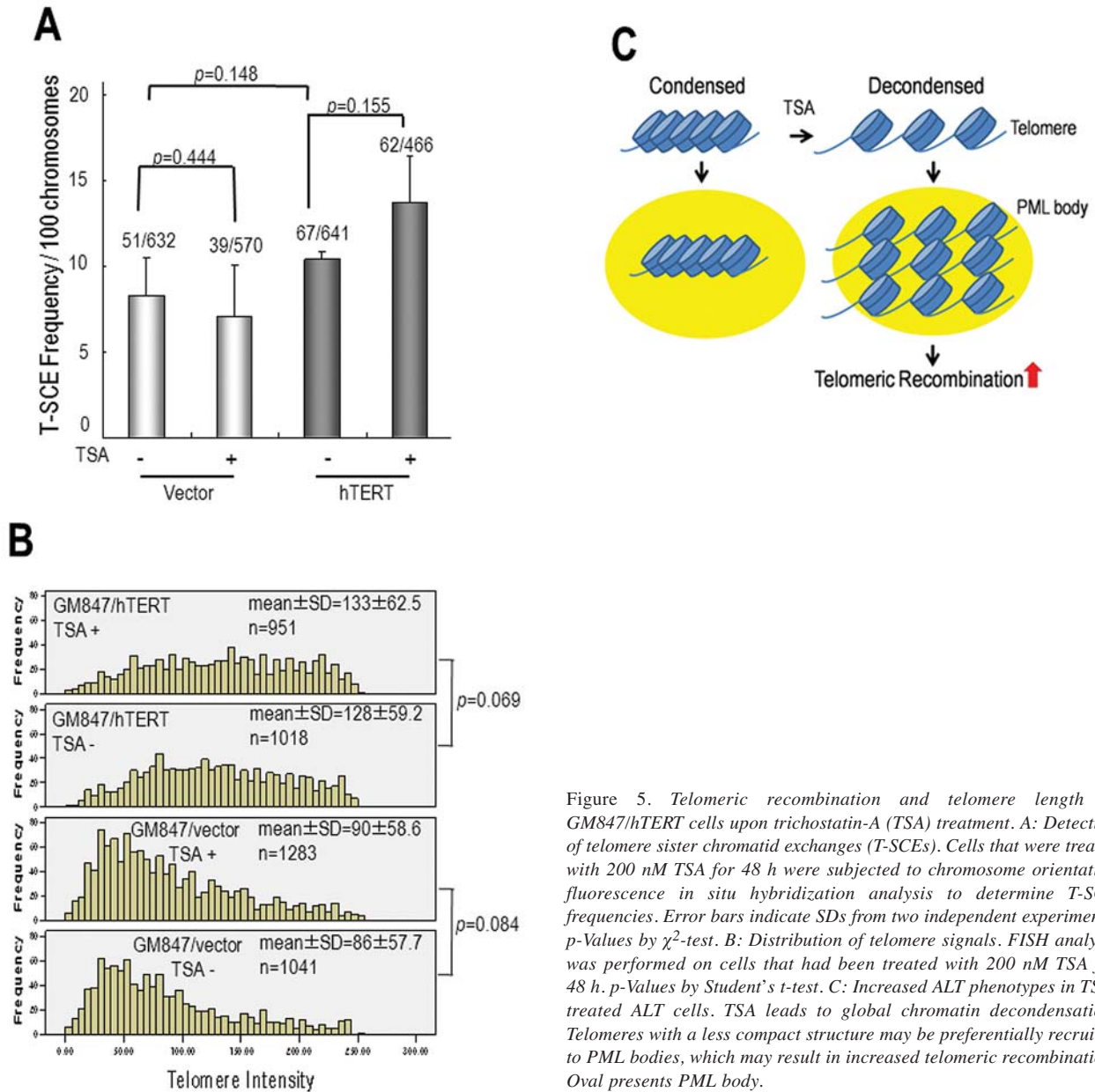


Figure 5. *Telomeric recombination and telomere length in GM847/hTERT cells upon trichostatin-A (TSA) treatment. A: Detection of telomere sister chromatid exchanges (T-SCEs). Cells that were treated with 200 nM TSA for 48 h were subjected to chromosome orientation fluorescence in situ hybridization analysis to determine T-SCE frequencies. Error bars indicate SDs from two independent experiments. p-Values by χ^2 -test. B: Distribution of telomere signals. FISH analysis was performed on cells that had been treated with 200 nM TSA for 48 h. p-Values by Student's t-test. C: Increased ALT phenotypes in TSA-treated ALT cells. TSA leads to global chromatin decondensation. Telomeres with a less compact structure may be preferentially recruited to PML bodies, which may result in increased telomeric recombination. Oval presents PML body.*

smaller fraction of the cells were APB-positive (18/100) and most APB-positive cells (17/18) contained fewer than five APBs per cell (Figure 3B and C). T-SCE events were also found to be more frequent in the TSA-treated cells (233/682, 34%), unlike in untreated cells (102/721, 14%; Figures 3D and E). The telomere length remained unchanged after 48 h of TSA treatment (Figures 3F and G). Our results for the WI38VA13 cells upon TSA treatment were quite similar to those for the GM847 cells, revealing that TSA induced the formation of APBs and T-SCEs in the ALT cells, but *hTERT* mRNA and telomere length remained unaffected.

Introduction of telomerase expression suppresses TSA-mediated ALT phenotype enhancement. One question that may arise is whether telomerase expression in ALT cells can cause changes in ALT phenotypes after TSA treatment. GM847 cells that stably expressed *hTERT* were established and confirmed by detecting *hTERT* protein expression, strong telomerase activity, and telomere elongation in GM847/hTERT cells (data not shown). In the GM847/hTERT cells, the induction of histone acetylation started at 100 nM TSA, and the induction level was maintained at 200 nM (Figure 4A). In the GM847/vector cells, however, histone

acetylation was actually induced at 200 nM. Thus, the condition for TSA treatment was set to 200 nM for 48 h (Figure 4A). With TSA treatment, the *hTERT* mRNA remained undetected in the GM847/vector cells, but increased in the GM847/*hTERT* cells (Figure 2), showing that TSA induced exogenous *hTERT* gene expression while GM847/vector cells remained telomerase-negative.

Analysis of FISH, combined with immunostaining revealed that TSA treatment increased APBs in both the GM847/*hTERT* and GM847/vector cells; however, the increase was smaller in the GM847/*hTERT* cells (Figures 4B and C). In the case of the GM847/vector cells, TSA treatment increased the number of APB-positive cells by 2.1-fold; APB-positive cells were found to compose 71% with TSA treatment and 34% without TSA treatment. In the case of the GM847/*hTERT* cells, the number of APB-positive cells increased only by 1.3-fold with TSA treatment (Figure 4C).

Incidence of T-SCEs was increased slightly, by 1.3-fold in GM847/*hTERT* cells after TSA treatment, which was statistically insignificant ($p=0.155$; Figure 5A). In the GM847/vector cells, TSA treatment yielded no significant change in T-SCEs ($p=0.444$; Figure 5A), which differed from the results for the parental GM847 cells where T-SCEs increased by nearly 2-fold (Figure 1E). It is not clear why different results were observed in the T-SCE analysis with the parental GM847 cells and the GM847/vector cells. Characteristics of GM847/vector cells might be slightly changed. In fact, the condition of TSA treatment for histone acetylation differed: 100 nM of TSA for the parental GM847 cells and 200 nM of TSA for the GM847/vector cells. Nevertheless, if we compare the data only from parental GM847 and GM847/*hTERT* cells, *hTERT* expression seemed to suppress TSA-mediated T-SCE events in the GM847/*hTERT* cells.

We also measured the telomere length of the GM847/*hTERT* and GM847/vector cells through Q-FISH analysis and found no noticeable changes in length under TSA treatment (Figure 5B). Although *hTERT* mRNA expression was up-regulated in the TSA-treated GM847/*hTERT* cells, changes in the telomere length were not noticed. Consistent with the results for the GM847 and WI38VA13 cells, noticeable changes in the telomere length may not have occurred during 48 h of TSA treatment.

Discussion

The state of chromatin is closely associated with telomere length regulation in telomerase-positive cells. However, the relationship between the state of chromatin and ALT phenotype has not been investigated in ALT cells. In this study, we observed that the treatment of ALT cell lines with TSA increased the number of APBs, enlarged some APBs, and enhanced the frequency of T-SCEs.

Previous reports showed that treatment of human cancerous cells with TSA results in histone hyperacetylation, which leads to global chromatin relaxation (11, 12). Although telomeric chromatin status was not examined in this study, TSA-induced histone acetylation supports the possibility of telomeres existing in a less compact structure. The results of the telomere length analysis and APB formation suggested that strong telomere spots that were found at the PML bodies of the TSA-treated cells were unlikely to be due to lengthened telomeres. Given the emergence of strong telomere spots in the PML bodies and increased T-SCEs upon TSA treatment, we expected that TSA-induced chromatin relaxation facilitated telomere assembly at PML bodies. In particular, telomeres with a less compact structure might have been preferentially recruited to PML bodies by the proteins that are required for telomeric recombination (Figure 5C). Consistent with previous reports (7-10), our results suggested a close relationship between telomeric recombination and chromatin relaxation.

GM847, GM847/vector, and GM847/*hTERT* cells that were not treated with TSA exhibited similar levels of APBs and T-SCEs, although a slight increase in APBs and T-SCEs was found in GM847/*hTERT* cells compared to GM847/vector, which was, however, statistically insignificant (Figures 1, 4, and 5). These results indicate that the introduction of telomerase into the GM847 cells did not alter the ALT phenotype, which is consistent with a previous report (19). Interestingly, telomerase expression in the GM847 cells seemed to suppress the TSA-mediated increase in APBs and T-SCEs. This may have been achieved by inhibiting telomere assembly at PML bodies. Previous reports suggest that telomerase prefers telomeres with less compact structures (20, 21). Our results also showed that the ALT mechanism favors telomeres with less compact structures. Therefore, in TSA-treated ALT cells with telomerase expression, the ALT mechanism may compete with telomerase for telomere maintenance.

In this study, we demonstrated that certain ALT phenotypes become more pronounced in TSA-treated ALT cells. Our findings provide important insights into telomere regulation in telomerase-negative cancerous cells. In future, it would be interesting to study this molecular mechanism in greater depth and to clarify how TSA-mediated chromatin relaxation facilitates telomeric recombination.

Acknowledgements

This research was supported by the Public Welfare & Safety Research Program through the National Research Foundation of Korea (NRF), for which funding by the Ministry of Education, Science and Technology (2010-0020841) was given to S.Y.R. It was also funded by grants from the NRF (2010-0008254 and 2011-0015638) that were directed to B.K.O. and partly by the Priority Research Centers Program through the NRF (2009-0093824), which were also directed to B.K.O.

References

- 1 Kim NW, Piatyszek MA, Prowse KR, Harley CB, West MD, Ho PL, Coviello GM, Wright WE, Weinrich SL and Shay JW: Specific association of human telomerase activity with immortal cells and cancer. *Science* 266: 2011-2015, 1994.
- 2 Bryan TM, Englezou A, Gupta J, Bacchetti S and Reddel RR: Telomere elongation in immortal human cells without detectable telomerase activity. *EMBO J* 14: 4240-4248, 1995.
- 3 Yeager TR, Neumann AA, Englezou A, Huschtscha LI, Noble JR and Reddel RR: Telomerase-negative immortalized human cells contain a novel type of promyelocytic leukemia (PML) body. *Cancer Res* 59: 4175-4179, 1999.
- 4 Bailey SM, Goodwin EH and Cornforth MN: Strand-specific fluorescence *in situ* hybridization: the CO-FISH family. *Cytogenet Genome Res* 107: 14-17, 2004.
- 5 Dunham MA, Neumann AA, Fasching CL and Reddel RR: Telomere maintenance by recombination in human cells. *Nat Genet* 26: 447-450, 2000.
- 6 Blasco MA: The epigenetic regulation of mammalian telomeres. *Nat Rev Genet* 8: 299-309, 2007.
- 7 García-Cao M, O'Sullivan R, Peters AH, Jenuwein T and Blasco MA: Epigenetic regulation of telomere length in mammalian cells by the Suv39h1 and Suv39h2 histone methyltransferases. *Nat Genet* 36: 94-99, 2004.
- 8 Benetti R, Gonzalo S, Jaco I, Schotta G, Klatt P, Jenuwein T and Blasco MA: Suv4-20h deficiency results in telomere elongation and derepression of telomere recombination. *J Cell Biol* 178: 925-936, 2007.
- 9 Gonzalo S, Jaco I, Fraga MF, Chen T, Li E, Esteller M and Blasco MA: DNA methyltransferases control telomere length and telomere recombination in mammalian cells. *Nat Cell Biol* 8: 416-424, 2006.
- 10 Vera E, Canela A, Fraga MF, Esteller M and Blasco MA: Epigenetic regulation of telomeres in human cancer. *Oncogene* 27: 6817-6833, 2008.
- 11 Bártová E, Pacherník J, Harnicarová A, Kovarík A, Kovaríková M, Hofmanová J, Skalníková M, Kozubek M and Kozubek S: Nuclear levels and patterns of histone H3 modification and HP1 proteins after inhibition of histone deacetylases. *J Cell Sci* 118: 5035-5046, 2005.
- 12 Tóth KF, Knoch TA, Wachsmuth M, Frank-Stöhr M, Stöhr M, Bacher CP, Müller G and Rippe K: Trichostatin A-induced histone acetylation causes decondensation of interphase chromatin. *J Cell Sci* 117: 4277-4287, 2004.
- 13 Park LH, Zhao R, West JA, Yabuuchi A, Huo H, Ince TA, Lerou PH, Lensch MW and Daley GQ: Reprogramming of human somatic cells to pluripotency with defined factors. *Nature* 451: 141-146, 2008.
- 14 Jiang WQ, Nguyen A, Cao Y, Chang AC and Reddel RR: HP1-mediated formation of alternative lengthening of telomeres-associated PML bodies requires HIRA but not ASF1a. *PLoS One* 6: e17036, 2011.
- 15 Lansdorp PM, Verwoerd NP, van de Rijke FM, Dragowska V, Little MT, Dirks RW, Raap AK and Tanke HJ: Heterogeneity in telomere length of human chromosomes. *Hum Mol Gene* 5: 685-691, 1996.
- 16 Al-Wahiby S, Wong HP and Slijepcevic P: Shortened telomeres in murine scid cells expressing mutant hRAD54 coincide with reduction in recombination at telomeres. *Mutat Res* 578: 134-142, 2005.
- 17 Zhong ZH, Jiang WQ, Cesare AJ, Neumann AA, Wadhwa R and Reddel RR: Disruption of telomere maintenance by depletion of the MRE11/RAD50/NBS1 complex in cells that use alternative lengthening of telomeres. *J Biol Chem* 282: 29314-29322, 2007.
- 18 Potts PR and Yu H: The SMC5/6 complex maintains telomere length in ALT cancer cells through SUMOylation of telomere-binding proteins. *Nat Struct Mol Biol* 14: 581-590, 2007.
- 19 Cerone MA, Londono-Vallejo JA and Bacchetti S: Telomere maintenance by telomerase and by recombination can coexist in human cells. *Hum Mol Genet* 10: 1945-1952, 2001.
- 20 Hemann MT, Strong MA, Hao LY and Greider CW: The shortest telomere, not average telomere length, is critical for cell viability and chromosome stability. *Cell* 107: 67-77, 2001.
- 21 Benetti R, García-Cao M and Blasco MA: Telomere length regulates the epigenetic status of mammalian telomeres and subtelomeres. *Nat Genet* 39: 243-250, 2007.

Received December 9, 2012

Revised January 21, 2013

Accepted January 22, 2013